Available online at www.sciencedirect.com
ScienceDirect
Solid-State Electronics 52 (2008) 649–656
SOLID-STATE ELECTRONICS
www.elsevier.com/locate/sse

Variation and mismatch effects of the low-temperature poly-Si TFTs on the circuit for the X-ray active matrix sensor

Ya-Hsiang Tai [a,*], Shih-Che Huang [b], Ko-Ching Su [b], Chen-Yeh Tseng [a]

[a] Department of Photonics and Display Institute, National Chiao Tung University, Hsinchu 30010, Taiwan, ROC
[b] Department of Photonics and Institute of Electro-Optical Engineering, National Chiao Tung University, Hsinchu 30010, Taiwan, ROC

Received 22 February 2007; received in revised form 25 November 2007; accepted 1 December 2007
Available online 29 January 2008

The review of this paper was arranged by Prof. S. Cristoloveanu

Abstract

The application of the capability of low-temperature poly-Si TFT circuits for high resolution X-ray active matrix sensor is explored. The integration of poly-Si TFT circuits on the glass enables an easy connection for the sensor array with fine pixel pitch. A novel charge sensitive amplifier circuit employing poly-Si TFTs is proposed for the readout system of the active matrix sensor. It can considerably increase the circuit's immunity to the unavoidable threshold voltage variations of the poly-Si TFTs. The V_{TH} mismatch effect of the TFTs, which results in the offset voltage of the charge amplifier, can also be suppressed by the proposed circuit. However, the noise arisen from the V_{TH} mismatch can be even larger than that from the V_{TH} variation after compensation. It reflects that, for higher bit digital X-ray image sensors, the mismatch effect of the devices must be properly taken into consideration.

Keywords: Charge sensitive amplifier; Poly-Si TFTs; X-ray active matrix sensor

1. Introduction

Active matrix sensor (AMS) technology is becoming attractive in a range of different applications, such as digital cameras and X-ray imaging systems [1–5]. In AMS applications, a system is required to read out the information sensed at each pixel location. This paper focuses on the readout circuitry of large area X-ray sensors used in diagnostic medical imaging such as radiography and mammography (static medical imaging) and fluoroscopy (dynamic imaging). The new AMS technology has the potential to fully replace film based analog technology and to make the system instantly available for use and diagnostic by radiologist.

In these applications, the active matrix is based on a two-dimensional array of amorphous silicon (a-Si) or polycrystalline silicon (poly-Si) pixels. The basic elements of each pixel contain the X-ray detector and thin film transistors (TFTs). Pixel signals are read out using analog circuitry. Conventional designs use single crystal ICs externally connected to the matrix sensor for reading the stored information. These external connections are often the reason for sensor malfunctions, such as loss of signal and increase of noise. Furthermore, they increase the cost of the panel.

In order to improve the sensor resolution and integrate system for reducing the whole system cost, integration of some (if not all) of the readout circuitry on the glass itself is desired. From the viewpoints of process integration, the single crystal Si technique may not be integrated on the same glass substrate with the active matrix sensors. On the other hand, using the IC bonding on the outside corner though may as well provide good electrical behaviors for the readout circuits, this may build difficulties and reduce

* Corresponding author. Address: Rm. 414, CPT Building, National Chiao Tung University, 1001 Ta Hsueh Road, Hsinchu 300, Taiwan, ROC. Tel.: +886 3 5131307; fax: +886 3 5737681.
E-mail address: yhtai@mail.nctu.edu.tw (Y.-H. Tai).

0038-1101/$ - see front matter © 2007 Elsevier Ltd. All rights reserved.
doi:10.1016/j.sse.2007.12.005

the reliability as the pixel size scaling down. In other words, IC package may not support the need for finer pitch AMS and larger area applications.

The integration may hence only be possible in either a-Si or low-temperature poly-Si technology, as single crystal Si (c-Si) cannot be deposited onto glass. A-Si TFTs have very low field mobility and requires larger driving voltages to form integrated circuits. On the other hand, poly-Si TFTs have superior properties compared to a-Si TFTs and are therefore more suitable for this application. However, poly-Si TFTs have poor uniformity and suffer from serious variation due to the narrow laser process window in producing large grain poly-Si thin film. The fluctuation of pulse-to-pulse laser energy and non-uniform laser beam profile makes it difficult for every laser shot to hit the super lateral growth regime on the whole glass. This results in the random grain boundary locations and traps exist in the channel region [6]. This will lead to many problems in real product applications such as output variation in analogue circuit. Since the device-to-device uniformity is difficult to control, it would be essential to develop circuits to compensate the device variation. In addition, the circuit design has to take into account the fact that adjacent transistors may not be perfectly matched [7] and hence some schemes for the cancellation of the mismatch effect should be applied.

Similar applications for poly-Si TFTs utilized for the integrated circuits can also be found in the application of the AMOLED (Active Matrix Organic Light-Emitting Diodes) display driven by the poly-Si TFTs. Since the late 90s, various methods are proposed to compensate the effect of device variation and increase the immunity to the device variation in the pixel circuits. Main methods are the capacitance compensation method [8,9], match TFT driving method [10], current mirror method [11], and current scaling method [12]. Though the poly-Si TFTs can be used to form both the circuits for display pixels and medical imaging, these two systems have very different requirements for the circuits. For the display pixels, it emphasizes the frame time and color for the human brain perception, while in the medical imaging system a very high precision and resolution for the sensed image is desired. In real applications for X-ray sensor, in order to achieve the high resolution of the sensed picture, the pitch for the pixels can be as low as 30 um, which is much smaller than that in the display applications. The smaller pitch also brings designers tougher task to devise the readout circuit to retrieve the precise data. Therefore, though for both applications the circuits could all be realized by the poly-Si devices, because of their different attributes the effect of device mismatch on the display and medical imaging system should be, respectively, examined. In the open literature, the effect of poly-Si device variation on the display system has been extensively studied for the AMOLED applications [8–12], while there are very few papers discussing the effect on the sensor system. In order to examine the effect of device variation on the medical imaging system and devise the corresponding compensation circuits, a thorough study is desired.

In the X-ray readout system, a charge sensitive amplifier (CSA) is required to enlarge the signal from the pixel array. In this paper, a poly-Si TFT CSA circuit that can be used for readout stored signals in active matrix X-ray sensors is proposed. Firstly, in Section 2, the standard sensor system architecture is described. The multiplexer circuit using poly-Si TFTs is also introduced. In Section 3, conventional CSA and the principle of storing and reading out the charge information is explained. A new circuit design of the operational amplifier in poly-Si TFT technology and its operating principle are presented. Mismatch effect and a method of offset cancellation are given in Section 4. Conclusions are provided in the final section.

2. System architecture

The AMS block diagram is shown in Fig. 1. The core pixel array consists of photodiode active pixels, which are accessed in the row-wise fashion using the scan driver. The X-ray signal is transformed by the photodiode and stored in the charge domain. All pixel charges in the row are read out into column analog readout circuits in parallel. Because of the high resolution and the fine pixel, the multiplexer is used to reduce the connection number and increase the pitch. The CSA provides a fixed value of gain for the column charges being read in the voltage domain using the column select logic. Each of the column-parallel readout circuits performs correlated double sampling (CDS) functions [13] to eliminate pixel offset variations and pixel noise. The analog-to-digital converter (ADC) generates the digital output according to the amplified signal for the subsequent processing and storage.

In this paper, the simulation is based on a p–i–n type photodiode [14], whose cross-section view and simple equivalent circuit in pixel are shown in Fig. 2a and b, respectively. The detector consists of an a-Si:H p–i–n photodiode and a stacked dielectric layer between the p-layer and its electrode as the main charge storage element. The

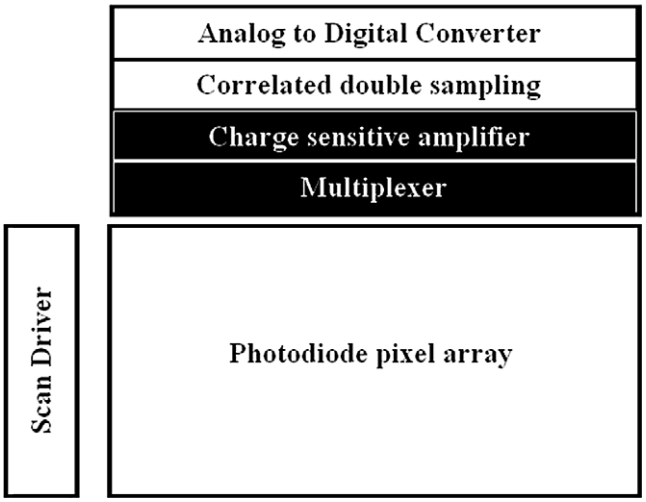

Fig. 1. The block diagram of the active matrix sensor system.

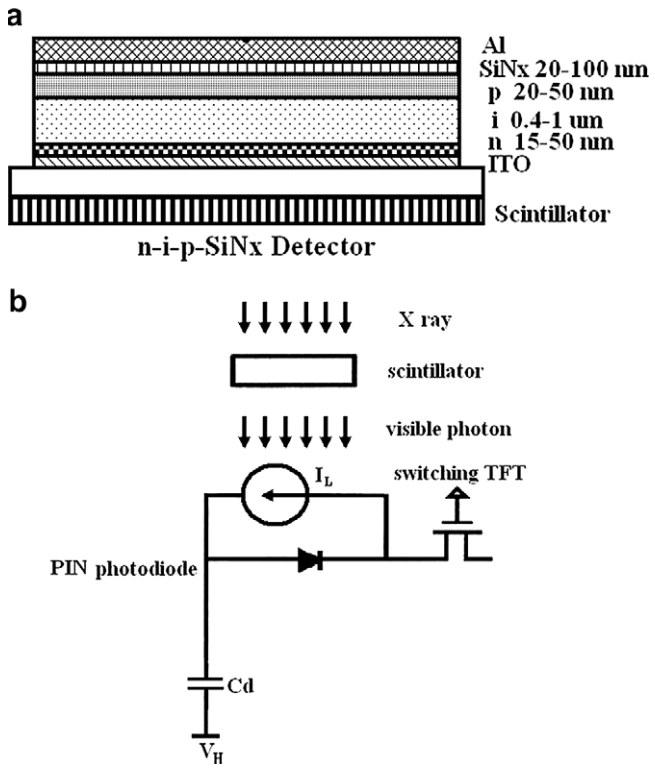

Fig. 2. (a) The cross-section view, and (b) the simple equivalent pixel circuit of the p–i–n photodiode.

Cd in the equivalent circuit is the insulator capacitance formed by the SiN_x layer, while the diode and the current source represent the p–i–n diode with the current generated by light.

Connecting to the pixel array, a 4:1 multiplexer is used to reduce the readout circuit required and enlarge their layout pitch. This multiplexer is made of transistors MN1 to MN4 as the main switches to select the four inputs as shown in Fig. 3. When high voltage signal is applied to the gate electrode of the n-type TFT, the switch will be turned on and then the input signal is able to transmit through. Besides, transistors MN5 to MN12 are the "dummy" switches for the charge injection cancellation [15].

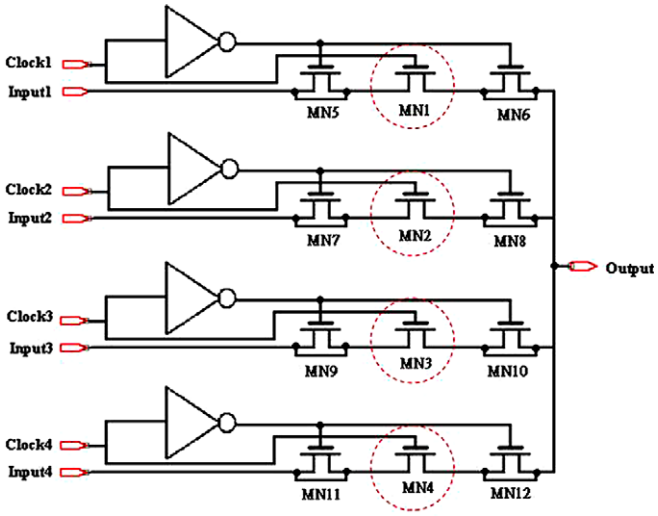

Fig. 3. The 4:1 multiplexer with dummy TFTs for AMS.

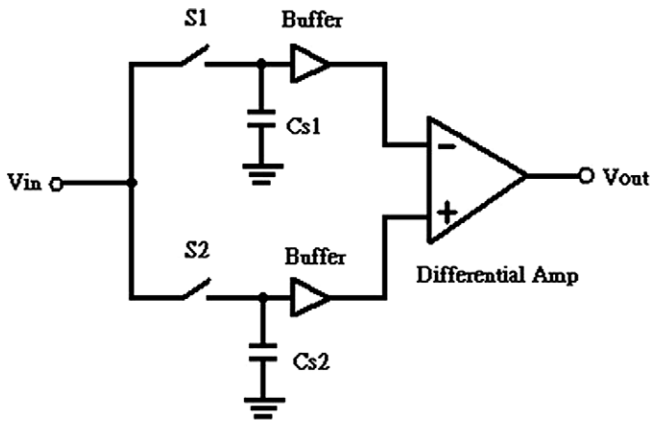

Fig. 4. The schematic view of correlated double sampling (CDS).

After the signals passing through the multiplexer, the CSA provides a fixed transform for the column charges to the voltage signal being read using the column select logic. The detailed operation of CSA would be discussed in Section 3. Output of CSA is fed to CDS, whose schematic is shown in Fig. 4. The operation of CDS includes two steps: At the first step, signal retaining information about offset, thus the background noise and reset noise are stored on the sampling capacitor Cs1. At the second step, the voltage which contains the pixel signals, as well as the noise and offset components in the sampling steps, is stored onto the other capacitance Cs2. The differential amplifier subtracts these two sampled signal to eliminate common noise components from the pixel information signal to get the pure pixel signal voltage and then delivers it to ADC. Since the output signal is amplified and the pitch is enlarged after CSA, CDS and ADC may use ICs externally connected, and can as well be integrated onto glass substrate with poly-Si TFTs.

3. Charge sensitive amplifier

Referring to Fig. 5a and b, the conventional process of reading the charge information from the detector capacitance Cd to CSA voltage output is conducted in the following way [14]:

In the initialization period, the charge previously stored on capacitance Cd would be released beforehand. When the switching TFT turns on, V_{ref} is set at low voltage V_L so that the photodiode is in forward bias and thus the pixel voltage V_c is discharged toward V_L till a voltage difference across the photodiode reaches its threshold voltage.

After the initialization period, sensors in the whole matrix are exposed to X-rays and the charges sensing the

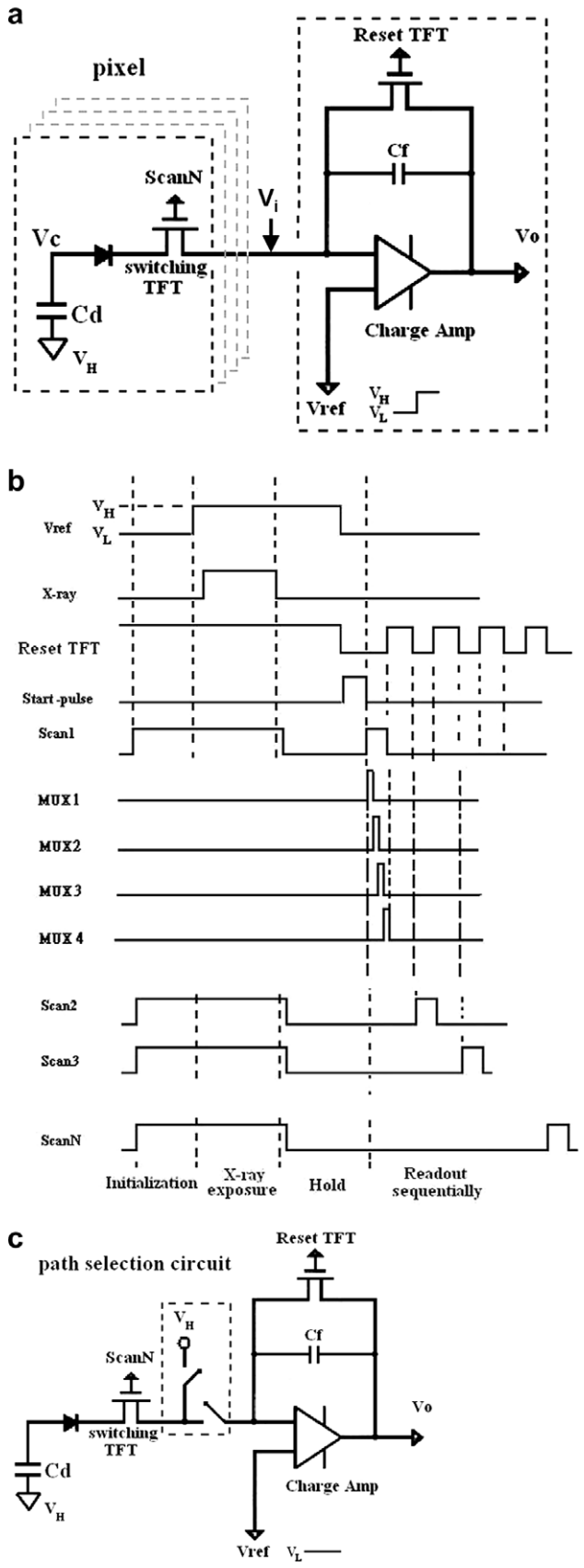

Fig. 5. (a) The conventional circuit, (b) the timing chart, and (c) the circuit with path selection circuit of the readout operation of charge sensitive amplifier in a sensor pixel.

X-ray image are stored on Cd in the pixel array. During this period, V_{ref} turns to high voltage V_H and thus the p–i–n diode is reverse-biased for the pile-up of the sensed charges from the photodiode and blocks the conduction between pixels and the data bus. After exposure, all the switching TFTs are turned off to isolate the pixel charge from CSA and the charges are held in Cd. After the readout time T_R, the signal is to be read. In this work T_R is set as 40 ms [14]. In the readout period, the switching TFTs are turned on row-by-row to read out the charge information from the matrix. In this work, a 4:1 multiplexer is adopted to relieve the issue of routing space limit of the data bus. Within each row-wise data readout, the multiplexer provides sequentially the clock 1, 2, 3 and 4, as shown in Fig. 5b, which corresponds to the clock in Fig. 3. Before each row-wise readout operation, the CSA is reset by turning on the reset TFT. Then, V_{ref} goes back to V_L and the photodiodes are in forward bias again. Therefore, the stored charges in a row are transferred from Cd onto the CSA feedback capacitance C_f, resulting in the output voltage V_o.

For such a conventional CSA configuration to be adapted in poly-Si TFT circuit, V_{ref} would toggle between V_H and V_L. The amplifier suffers from the high supply voltage, which leads to higher power consumption and worse TFT device degradation. Therefore, a path selecting circuit is inserted before the input of CSA as shown in the Fig. 5c. It requires two additional switches and one voltage source V_H to supply reverse-bias voltage of diode if required. Thus, V_{ref} can be fixed at V_L and the supply voltage could be reduced.

For the kind of p–i–n photodiode stacked with a SiN_x dielectric capacitor layer with typical thickness of 60 nm, dielectric constant of 6.59 and area of 100 μm × 100 μm, the corresponding detector capacitor C_d is about 10 pF. The sensitivity of the X-ray sensor is assumed to be 1–3 μCoul/cm^2 R. For a usual exposure dose of 100–600 mR/s and exposure time of 40–200 ms [14], the injection of charge signal would be several pico-coulombs. The detector capacitance C_d and the feedback capacitance C_f selected as 10 pF and 2 pF, respectively, which provides a gain of −5. Though different exposure time durations may lead to different charge signals in the pixel, the method proposed in this paper would still be applicable.

As an example, for the sensed charge of 2pC stored on Cd, the input signal V_{in} for the CSA will be 0.2 V. It corresponds to the CSA output signal of −1 V, which will be added to the reference voltage V_{ref} of 7 V. Thus, the ideal output voltage of CSA should be 6 V.

To study the effect of the poly-Si TFT device variation on circuit uniformity, Monte Carlo simulation method is executed. This method treats the device parameter distribution as the Gaussian distribution and randomly picks a value for each device in each simulation. Via this method, only the mean value and the standard deviation value of the device parameters are required to simulate the output fluctuation due to the device variation. The detailed description to this

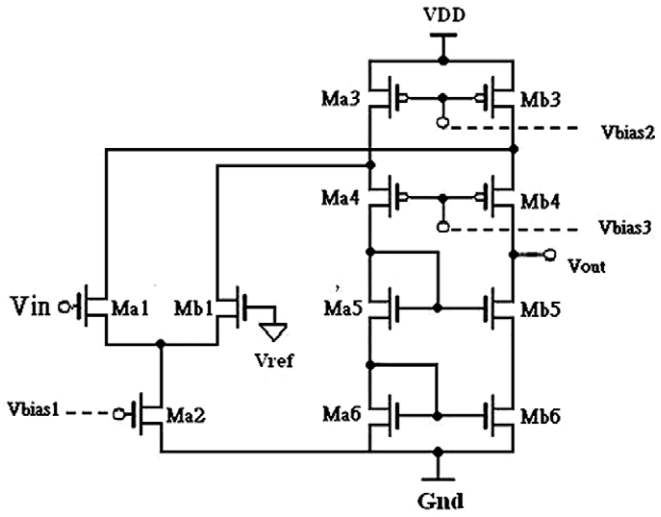

Fig. 6. A folded-cascode operation amplifier used for CSA.

method can be found in Ref. [16]. According to the measurement database, the threshold voltage V_{TH} distributions of the TFTs are with the mean values of 1.6 V for n-type and −1.3 V for p-type and the deviation for both types is 1 V. The schematic of a folded-cascode operation amplifier used for CSA is shown in Fig. 6 [17]. As can be seen, many TFT pairs are used and represented by Ma*n* and Mb*n*. They are assumed to be perfectly matched in this section. Thirty times of Monte Carlo simulation results of the output waveform are shown in Fig. 7a. It can be observed that the output waveforms exhibit severe variation after 40 ms, which is the time for the signal to be retrieved from the circuit. The diverse behaviors can be attributed to the V_{TH} variation of the TFTs. Therefore, the drain currents of the TFTs can be very different, and the output voltage of CSA would largely deviate from the ideal output voltage 6 V.

In order to diminish the effects of the device variation, the circuit shown in Fig. 8a is proposed in this work to replace the fixed bias voltage for the n-type TFT. A diode-connected TFT, a capacitor Cvt and two switches S1 and S2 are used. The TFT is also assumed to match the corresponding TFT to be biased. The operation consists of two periods. In the first period, only S1 turns on and S2 is open so that a high voltage VDD is stored in Cvt. In the second period, S1 is open and S2 turns on to discharge the stored voltage to $(V_{bias1} + V_{TH})$, which makes the new bias voltage V'_{bias1} compensate the V_{TH} variation. Similarly, the bias voltage on the p-type TFTs can be compensated by the circuit shown in Fig. 8b. Another 30 times of Monte Carlo simulation with the same V_{TH} distribution and simulation setup for the output voltage of the new CSA with compensation circuit is shown in Fig. 7b. It can be seen that for the output voltage the immunity to the device variation can be greatly improved and its non-uniformity range in the CSA output voltage can be reduced to as low as 0.08 V.

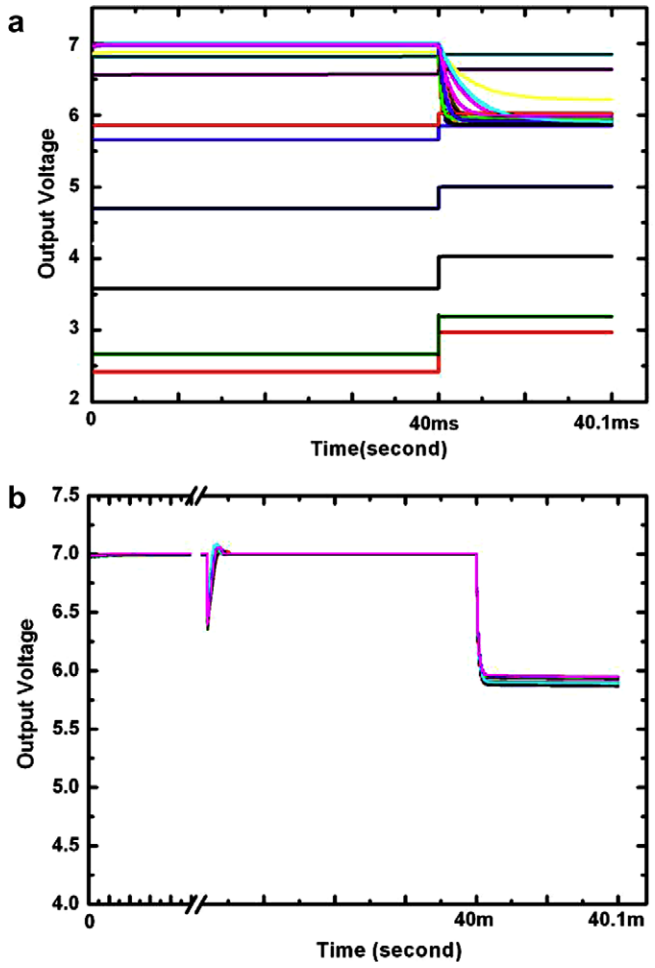

Fig. 7. Thirty times Monte Carlo simulation results for CSA output voltage of the (a) conventional circuit, and (b) circuit with the compensation method.

Fig. 9a shows the output voltages of the new CSA with respect to the different input signals. A good linearity between the output voltage and input signal is obtained and it is immune to variation. Fig. 9b compares the standard deviations of the output voltages for the circuits with different bias voltage compensations. The merits of the proposed circuit are apparent that the wide operation range and the small deviation below 0.033 V can be obtained. Furthermore, the deviation is less dependent on the input voltage, reflecting the effectiveness of the proposed circuit.

4. Mismatch effect

With the method in the previous section, the circuit's immunity to the threshold voltage variation is considerably improved. However, even if the two devices are very-closely placed, the micro variation is still observed as shown in Fig. 10 [13]. The proposed circuit utilizes the assumption that the devices are perfectly matched, whose immunity behavior may be deteriorated as the mismatch effect takes place. To understand the effect of device mismatch, a fur-

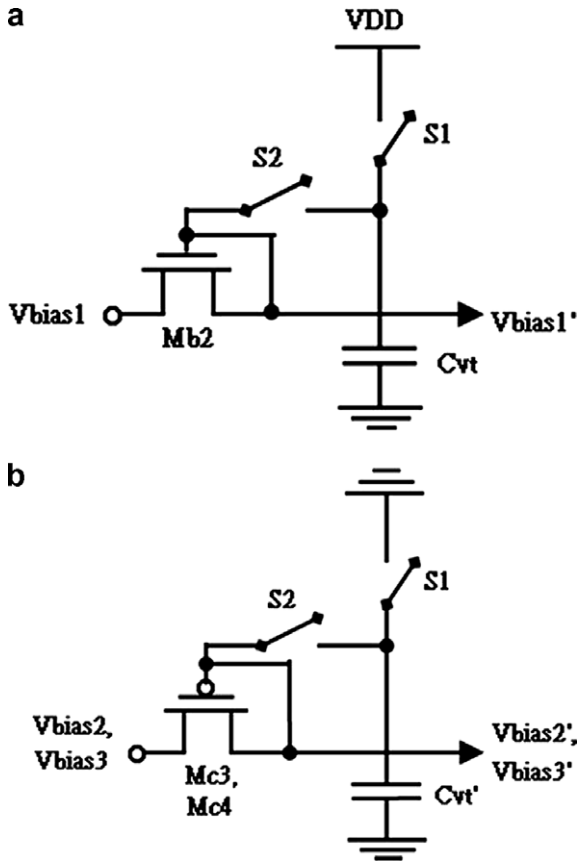

Fig. 8. Compensation circuits of the bias voltages for (a) n-type and (b) p-type TFTs.

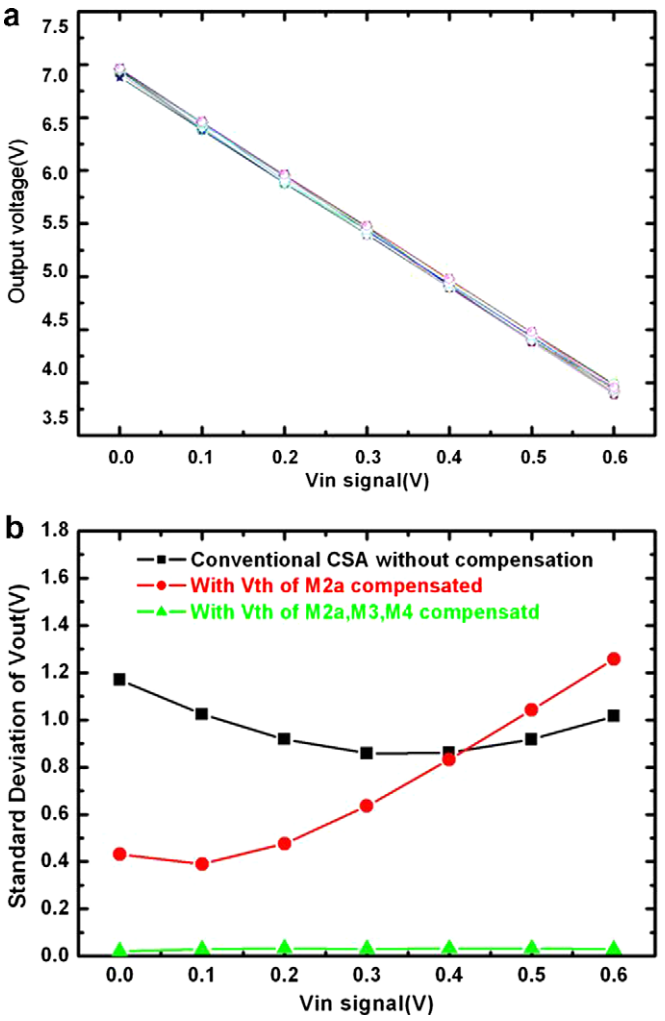

Fig. 9. Thirty times Monte Carlo simulation results of (a) output voltage with respect to the different input signal and (b) comparison of the circuits with different bias voltage compensation methods.

ther study is of practical interest and necessity. For simulation, offset voltage V_{OS} is put at the input node to represent the V_{TH} mismatch of the TFT pair. The output voltage in the period before the X-ray exposure is simulated to examine the offset noise. Fig. 11 shows the statistical simulation results with V_{ref} set at 7 V. The device parameters used in simulation are shown in Table 1, which are based on the real measured data of the very-closely located devices [18,19]. The device mismatch ratio is defined as three times of the standard deviation divided by its mean value. Referred to Fig. 11, the output voltage with TFT mismatch behavior and offset voltage V_{OS} exhibits a large variation range from 6.75 V to 7.2 V. The large range around 0.55 V could lead to the inaccuracy of the retrieved data and thus the compensation circuit to suppress the mismatch effect is required.

The circuit shown in Fig. 12a is used to cancel the offset voltage. The region surrounded with dashed line represents the operation amplifier with the offset voltage V_{OS}. This circuit corresponds to the right side of the whole CSA circuit shown in Fig. 5a. The proposed circuit utilizes three additional transistors and a capacitor to cancel the effect of offset. The operation of the circuit contains two stages. Firstly, only switches T1 turns on to make the signal V_{OS} stored in the capacitor C_{st}, as shown in Fig. 12b. At this time, the

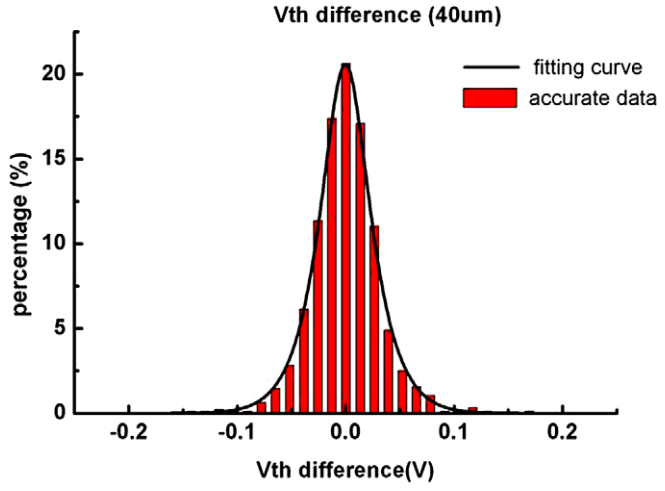

Fig. 10. The distribution of V_{TH} difference between two TFTs with device interval 40 um.

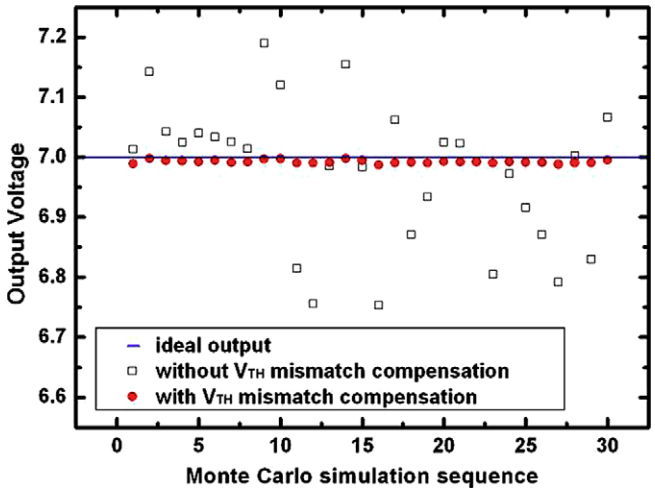

Fig. 11. Thirty times Monte Carlo simulation results for the output voltages of CSA in the period before X-ray exposure.

Table 1
The device parameters used in simulation for describing the mismatch behavior in section IV

	V_{TH} (V)	Mu (V/dec)
n-Type		
Mean value	1.69	59.66
Standard deviation	0.03	7.84
Mismatch ratio	0.053	0.394
p-Type		
Mean value	2.41	75.31
Standard deviation	0.05	2.29
Mismatch ratio	0.062	0.091

voltage at node V_{in}^{+} is equal to V_{ref} plus V_{OS}. Secondly, T1 is turned off and only T2 turns on, as shown in Fig. 12c. At this time the voltage across the capacitor would be V_{ref} and ($V_{ref} - V_{OS}$), making the voltage at the node V_{in}^{+} is V_{ref}, which could be free from the effect of V_{OS}. With this compensation, variation between V_{out} and V_{ref} can be reduced to 0.02 V, as shown by the solid circles in Fig. 11.

Furthermore, the mismatch effect with different input signals is shown in Fig. 13. As can be seen, for the circuit without V_{TH} mismatch compensation, the standard deviation of the output voltage can be as high as 0.8 V and decreases with input signal to around 0.6 V. However, the standard deviation of output voltage with V_{OS} compensation is all below 0.08 V and slowly increases with the input signal. This reveals that the proposed circuit can effectively reduce the effect of device mismatch on the CSA sensor. Nevertheless, for the worst case, for the two compensation circuits the noise arisen from the V_{TH} mismatch effect is about three times larger than that from V_{TH} variation effect, which means that both the variation effect and the mismatch effect for the circuits are important and neither of them can be ignored. This also reveals that the device variation should be carefully taken into consideration for the real AMS applications.

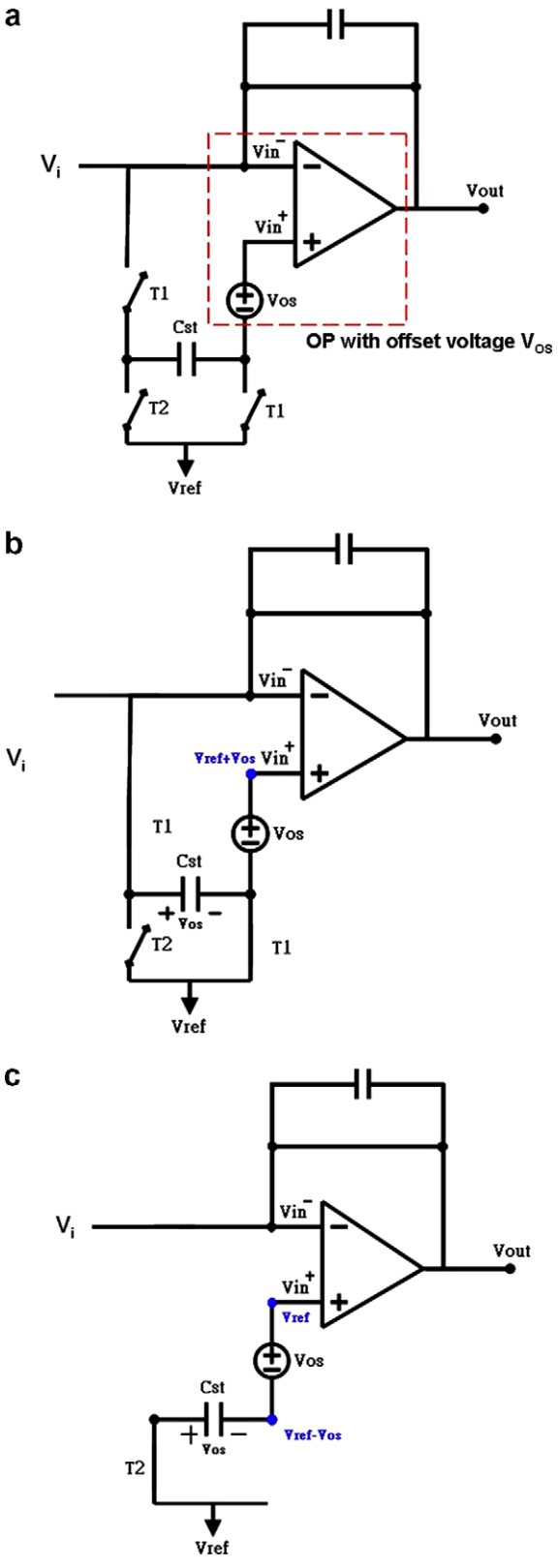

Fig. 12. (a) CSA circuit with input offset cancellation. The operation contains (b) the capacitor compensation stage and (c) cancellation stage.

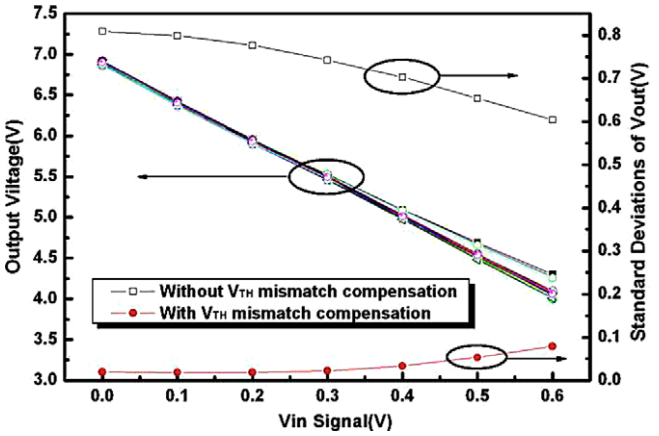

Fig. 13. Mismatch effect of the output voltage with respect to different input signal and comparison of the circuits with and without V_{TH} mismatch compensation.

5. Conclusion

A poly-Si TFT circuit with V_{TH} compensation and offset cancellation capabilities that can be employed in active matrix sensor systems has been presented and its operation is described and simulated base on the really measured database of device parameter. The proposed circuit can provide high immunity to the variation of poly-Si TFT characteristics and reduce the output voltage deviation to as low as 0.08 V. The effect of TFT mismatch is examined and it is found to be even larger than the variation effect for the circuit with compensation. A circuit utilizes three transistors and a capacitor is proposed to cancel the offset effect and the variation of the output voltage can be suppressed to below 0.1 V. This indicates that, for the digital X-ray image with higher resolution, the improvements of poly-Si TFT circuits in both device variation and mismatch control are required.

Acknowledgments

This work has been sponsored by the National Science Council, Republic of China (NSC 94-2218-E-009-026). This work was partially supported by MOEA Technology Development for Academia Project # 94-EC-17-A-07-S1-046. The technical support in the usage of simulation tools from Cadence is also acknowledged.

References

[1] Nathan A, Park B-K, Ma Q, Sazonov A, Rowlands JA. Amorphous silicon technology for large area digital X-ray and optical imaging. Microelectron Reliab 2002;42:735–46.
[2] Moy JP. Large area X-ray detectors based on amorphous silicon technology. Thin Solid Films 1999;337:213–21.
[3] Ryu JI, Won SH, Hur JH, Kim HJ, Jang J. Simulation of a novel amorphous silicon photoconductor array. J Korean Phys Soc 2001;39: S112–5.
[4] Izumi Y, Yamane Y. Solid state X-ray imagers. MRS Bull 2002;27(11):889–93.
[5] Weisfield RL. Amorphous silicon TFT X-ray image sensors. In: International Electron Devices Meeting IEDM 98 Technical Digest. San Francisco, CA, USA; 1998.
[6] Chan VWC, Chan PCH, Yin C. The effects of grain boundaries in the electrical characteristics of large grain polycrystalline thin-film transistors. IEEE Electron Devices 2002;49:1384–91.
[7] Huang SC, Chou YP, Tai YH. Statistical study on the states in the low-temperature poly-silicon films with thin film transistors. In: ICMCTF HP-19, 2006. p. 109.
[8] Jung SH, Park JH, Han CW, Han MK. New source follower type analog buffers using poly-Si TFTs for active matrix displays. In: SID Tech Dig, 2004. p. 1452–55.
[9] Choi SM, Kwon OK, Komiya N, Chung HK, A self-compensated voltage programming pixel structure for active-matrix organic light emitting diodes. In: IDW Tech Dig, 2003, p. 535–8.
[10] Jung SH, Nam WJ, Han MK. A new voltage-modulated AMOLED pixel design compensating for threshold voltage variation in poly-Si TFTs. IEEE Electron Device Lett 2004;25:690–2.
[11] Yeh YH, Shih JR, Chen CR, Kuo YH, Liu YL, Cheng CC, et al. A Uniform 10-inch color active-matrix OLED with new pixel driving circuit. In: IDW Tech Dig, 2003. p. 259–62.
[12] Lee JH, Nam WJ, Jung SH, Han MK. A new current scaling pixel circuit for AMOLED. IEEE Electron Device Lett. 2004;25:280–2.
[13] Rankov A, Rodriguez-Villegas E, Lee MJ. A novel correlated double sampling poly-Si circuit for readout systems in large area X-ray sensors. In: IEEE International Symposium, vol. 1, 2005. p. 728–31.
[14] Fann SS, Jiang YL, Hwang HL. Operating principles and performance of a novel a-Si:H p–i–n-based X-ray detector for medical image applications. IEEE Trans. Electron Device 2003;50(2):341–6.
[15] Lin HYu. Analog Integrated Circuits For Neuronal Signal Processing, M.S. State thesis, Dept. Electrical Eng, Stony Brook Univ., New York, USA, May 2003.
[16] Synopsys, Inc., HSPICE Simulation and Analysis User Guide, Version Y-2006.03, March 2006. p. 445–54.
[17] Lee TH, Hee GC, Seung JK, Lee W, Lee W, Han SH. Analysis of 1/f noise in CMOS preamplifier with CDS circuit. IEEE Trans Nucl Sci 2002;49(4):1819–23.
[18] Huang Shih-Che, Peng Guo-Feng, Chern Jyh-Long, Tai Ya-Hsiang. Statistical investigation on the variation behavior of low-temperature poly-Si TFTs for circuit simulation. In: SID Tech Dig, 2006. p. 329–32.
[19] Tai Y-H, Huang S-C, Chen W-P, Chao Y-T, Chou Y-P, Peng G-F. A statistical model for simulating the effect of LTPS TFT device variation for SOP applications. IEEE J Display Technol 2008;3(4):426–33.